

## THE ECLIPSING DOUBLE-LINED SPECTROSCOPIC BINARY SYSTEM V505 PERSEI

LAURENCE A. MARSCHALL

Department of Physics, Gettysburg College, Gettysburg, Pennsylvania 17325  
 Electronic mail: marschal@gettysburg.edu

ROBERT P. STEFANIK

Harvard-Smithsonian Center for Astrophysics, 60 Garden Street, Cambridge, Massachusetts 02138  
 Electronic mail: stefanik@cfa.harvard.edu

CLAUD H. LACY

Department of Physics, 226 Physics Building, University of Arkansas, Fayetteville, Arkansas 72701  
 Electronic mail: clacy@comp.uark.edu

GUILLERMO TORRES

Harvard-Smithsonian Center for Astrophysics, 60 Garden Street, Cambridge, Massachusetts 02138  
 Electronic mail: torres@cordoba.harvard.edu

DAVID B. WILLIAMS

9270-A Racquetball Way, Indianapolis, Indiana 46260  
 Electronic mail: Dbwilymuz@aol.com

FRANZ AGERER

Private Observatory, D-84184 Zweikirchen, Germany  
 Electronic mail: Agerer.Zweik@t-online.de

Received 1997 February 4; revised 1997 April 25

## ABSTRACT

The recently-discovered eclipsing double-lined spectroscopic binary V505 Persei (SAO 23229) consists of two nearly identical F5 main sequence stars in a 4.2 day orbit. We have obtained both spectroscopic and photometric observations of the binary that densely sample the complete cycle of radial velocity and light variations. These observations have been used to determine the elements of the orbit, to determine individual masses of the stars in the system to a precision of better than 1%, and to estimate an age for the system. The derived properties agree well with current stellar structure models and provide fundamental data for tests of stellar evolution theory. © 1997 American Astronomical Society.  
 [S0004-6256(97)00508-6]

## 1. INTRODUCTION

Although one might have thought that all the bright, large amplitude variable stars had been discovered long ago, a number of these systems have been found in recent years. Among these is the 7th magnitude eclipsing binary star SAO 23229 (V505 Persei; HD 14384;  $\alpha(2000.0) = 02^{\text{h}}21^{\text{m}}12.7^{\text{s}}$ ;  $\delta(2000.0) = 54^{\circ}30'36''$ ;  $V = 7.3$ ), whose sizable eclipses (0.5 mag in depth) were discovered by amateur astronomer Daniel Kaiser in 1989 September (Kaiser 1989; Kaiser *et al.* 1990; MacRobert 1990).

The initial observations of Kaiser suggested a photometric period of about 2.1 days. Subsequent spectroscopic observations at the Oak Ridge Observatory of the Harvard-Smithsonian Center for Astrophysics (Marschall *et al.* 1990) revealed that the system was a double-lined binary with two components of approximately equal luminosity, and that the reported 2.1 day period, half the true period of 4.2 days,

represented the time between nearly-equal secondary and primary eclipses.

Such double-lined eclipsing binary systems are our primary source of fundamental data on stellar masses and a powerful tool for testing theories of stellar structure and evolution (Andersen 1991; Latham *et al.* 1996). Since V505 Persei was so bright, it was clear that this could be a valuable target for a highly-precise mass determination. Therefore, in 1990, a program of spectroscopic radial velocity observations was begun by two of the authors (Marschall and Stefanik) at the Center for Astrophysics (CfA), while photometric observations were undertaken by two other authors (Williams and Agerer).

## 2. SPECTROSCOPIC OBSERVATIONS AND ANALYSIS

Sixty-three spectra of V505 Persei were obtained between 1990 February and 1992 August using CfA echelle spectrographs mounted on the 1.5 m Wyeth Reflector at the Oak

Ridge Observatory (ORO) in Harvard, Massachusetts, and (for three exposures) the 1.5 m Tillinghast Reflector at Fred L. Whipple Observatory (FLWO) in Amado, Arizona. The observations, which cover the spectral range 5165.77–5211.23 Å, were recorded using photon-counting intensified Reticon detectors which typically registered continuum levels of 100 counts per pixel in integrations of a few minutes. The instrument and the methods of data reduction used with the system are described by Latham (1985, 1992).

Radial velocities for the two components of V505 Per were derived from the CfA spectra by cross correlation, first using the program XCSAO within the NOAO IRAF<sup>1</sup> environment (Kurtz *et al.* 1992). The program derives radial velocities by correlating the stellar spectrum against a synthetic template spectrum chosen to match, as well as possible, the spectral characteristics of the program star.

The four free parameters for template spectra are effective surface temperature ( $T_{\text{eff}}$ ), surface gravity ( $\log g$ ), metallicity ( $\log[\text{Fe}/\text{H}]$ ), and rotational velocity ( $v \sin i$ ). We constrained two of these parameters,  $T_{\text{eff}}$  and  $\log g$ , using the published spectral type, F5 V, and we assumed solar metallicity,  $\log[\text{Fe}/\text{H}] = 0.0$ . There was, however, no value of  $v \sin i$  for V505 Per in the literature, though visual inspection of our spectra indicated that  $v \sin i$  was less than  $30 \text{ km s}^{-1}$ . Making the reasonable assumption that the rotation of a main sequence binary with a 4.2 day period is tidally synchronized to its period of revolution (Mathieu 1994), V505 Per should have an equatorial velocity of  $15 \text{ km s}^{-1}$ .

To test our choice of parameters, we derived radial velocities using a grid of template spectra of varying temperature, gravity, and rotational velocity. The strongest correlations were obtained with the effective temperature  $T_{\text{eff}} = 6500 \text{ K}$  and surface gravity  $\log g = 4.5$ , as expected for an F5 V. Though we had no template at the expected  $v \sin i = 15 \text{ km s}^{-1}$ , the best correlations, equally strong, were obtained using templates with  $v \sin i = 10 \text{ km s}^{-1}$  and  $v \sin i = 20 \text{ km s}^{-1}$ .

Velocities for a preliminary orbit were derived from the resulting correlations by fitting simple quadratic curves to the correlation peaks, and an orbital solution was calculated separately for each component to provide initial values for a simultaneous double-lined solution.

Blending of the correlation peaks can introduce serious systematic errors in the derived radial velocities of double-lined binary systems. To deal with this problem, radial velocities for a final orbit determination were derived using a version of the TODCOR correlation procedure developed by Mazeh & Zucker (1994), which effectively uses a two-dimensional cross correlation of the object spectrum against a template composed of the sum of the individual templates for each component. Because of the nearly identical appearance of the correlation peaks (and the nearly identical appearance of primary and secondary eclipses, presented in the next section), we used the same template for the secondary and the primary. The resulting radial velocities for primary

TABLE 1. Radial velocity measurements of V505 Persei.

Heliocentric Julian Day (240000+)	Phase	$V_p$ ( $\text{km s}^{-1}$ )	$V_s$ ( $\text{km s}^{-1}$ )	$V_p$ ( $\text{km s}^{-1}$ )	$V_s$ ( $\text{km s}^{-1}$ )	Telescope
		correlated against template $v \sin i = 10 \text{ km s}^{-1}$		correlated against template $v \sin i = 20 \text{ km s}^{-1}$		
47935.5048	0.058	-31.29	31.96	-31.69	32.18	ORO
47935.5980	0.080	-42.63	43.03	-42.26	43.40	ORO
47942.5068	0.717	86.60	-87.88	85.96	-86.89	ORO
47957.4789	0.263	-89.35	88.95	-88.98	88.91	ORO
47958.5562	0.518	10.30	-8.34	5.62	-2.67	ORO
47959.4759	0.736	87.50	-91.65	87.59	-90.83	ORO
47960.4978	0.978	12.66	-12.17	11.81	-12.37	ORO
47961.4984	0.215	-86.77	87.62	-86.22	88.05	ORO
47964.4805	0.921	43.24	-43.39	43.78	-43.49	ORO
47964.5875	0.947	30.04	-28.83	29.89	-29.35	FLWO
47965.4779	0.158	-73.03	75.39	-74.21	75.36	ORO
47965.5867	0.183	-81.19	82.37	-80.61	81.58	FLWO
47966.5887	0.421	-42.11	42.97	-41.88	42.91	FLWO
47989.5018	0.848	71.73	-73.40	71.62	-73.41	ORO
47990.4975	0.084	-44.24	45.17	-43.39	44.45	ORO
47991.5011	0.321	-78.85	81.61	-78.07	81.45	ORO
47994.5068	0.033	-17.27	18.59	-17.64	19.08	ORO
48145.6489	0.832	79.25	-78.34	77.69	-77.69	ORO
48160.6300	0.380	-62.03	62.15	-61.75	61.52	ORO
48165.8759	0.623	62.13	-62.63	61.45	-63.18	ORO
48166.6538	0.807	83.78	-85.33	82.09	-83.70	ORO
48167.5905	0.029	-14.32	16.36	-14.92	17.23	ORO
48189.8937	0.311	-83.16	84.10	-82.39	82.70	ORO
48192.8398	0.009	-6.20	7.34	0.11	0.14	ORO
48194.5642	0.418	-44.21	45.79	-44.86	46.09	ORO
48195.8824	0.730	87.13	-89.85	86.22	-88.52	ORO
48198.8136	0.424	-40.77	41.86	-41.09	42.34	ORO
48200.5277	0.830	78.49	-79.39	77.98	-77.65	ORO
48202.8097	0.371	-65.91	64.69	-65.97	63.87	ORO
48220.7416	0.618	58.33	-61.32	57.85	-62.46	ORO
48227.4984	0.218	-87.12	85.60	-85.14	85.80	ORO
48227.7213	0.271	-88.76	90.50	-89.86	88.84	ORO
48230.4993	0.929	39.95	-40.22	39.84	-40.47	ORO
48232.4465	0.390	-56.89	57.54	-57.33	56.71	ORO
48235.6998	0.161	-74.77	76.82	-75.05	76.84	ORO
48236.4538	0.339	-74.99	76.44	-75.57	76.54	ORO
48236.6690	0.390	-56.47	57.60	-56.80	56.39	ORO
48251.7412	0.960	22.90	-22.35	23.58	-22.69	ORO
48257.6918	0.370	-64.88	67.13	-65.44	65.97	ORO
48259.6705	0.838	75.26	-76.96	75.59	-77.30	ORO
48281.5457	0.019	-11.62	10.64	-9.69	8.58	ORO
48284.5646	0.734	88.30	-88.87	88.49	-89.55	ORO
48286.5793	0.212	-85.28	87.77	-86.04	86.41	ORO
48289.5645	0.919	42.17	-44.95	42.08	-46.29	ORO
48291.6178	0.405	-51.27	50.64	-52.03	50.41	ORO
48323.4980	0.956	23.95	-24.65	23.55	-25.58	ORO
48325.4958	0.429	-38.63	39.28	-39.07	38.53	ORO
48499.6894	0.688	83.50	-82.74	82.81	-83.28	ORO
48501.6728	0.157	-74.69	75.73	-74.37	75.22	ORO
48528.9069	0.608	54.68	-56.45	55.01	-55.74	ORO
48543.9317	0.167	-77.75	80.95	-76.74	79.75	ORO
48550.5843	0.742	88.65	-90.24	88.39	-89.78	ORO
48558.8284	0.695	83.25	-84.74	82.51	-85.16	ORO
48579.4538	0.580	42.61	-44.48	42.39	-44.60	ORO
48580.7917	0.897	53.56	-54.52	54.05	-55.41	ORO
48586.4459	0.236	-87.47	89.58	-87.79	88.97	ORO
48633.6425	0.415	-45.71	46.40	-46.17	45.29	ORO
48694.4774	0.824	80.33	-79.91	79.64	-79.58	ORO
48696.4773	0.298	-84.27	86.10	-83.90	85.57	ORO
48698.5171	0.781	87.96	-88.17	87.34	-88.43	ORO
48700.4929	0.249	-90.52	90.06	-91.85	89.72	ORO
48810.8156	0.379	-61.51	63.16	-61.87	62.58	ORO
48845.7320	0.649	71.89	-72.85	72.16	-73.42	ORO

and secondary are presented in Table 1. Column 1 of that table lists the HJD of observation, column 2 the phase determined from the orbital elements determined from the photometric solutions (see below); columns 3–6 the velocities derived from TODCOR assuming either  $v \sin i = 10 \text{ km s}^{-1}$  and  $v \sin i = 20 \text{ km s}^{-1}$ , and column 7 the site used for the observations (FLWO = Fred L. Whipple Observatory; ORO = Oak Ridge Observatory).

Orbital elements were derived from these radial velocities using an iterative fitting routine with the period of the iterative solution adopted from the photometric study (see below). Since initial solutions yielded eccentricities of order

<sup>1</sup>IRAF is distributed by the National Optical Astronomy Observatories, which is operated by the Association of Universities for Research in Astronomy under Contract with the National Science Foundation.

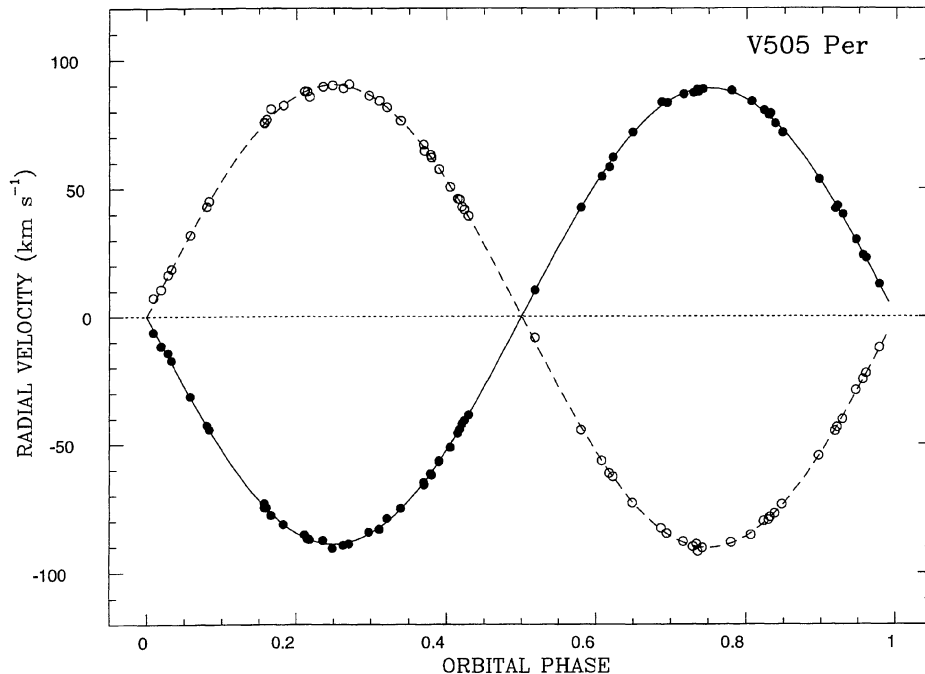


FIG. 1. Observed CfA radial velocities and computed orbits for V505 Per. The primary velocities used in the solutions are shown as filled circles and the secondary velocities used in the solution as open circles.

0.001, similar in size to its uncertainty, we chose to fix the eccentricity at zero in the final solutions. To see how sensitive the solutions were to the choice of initial conditions and the selection of data, we ran numerous orbital solutions, using different initial conditions and excluding more or fewer of the velocities derived from blended correlations. The orbital elements appeared quite robust, and ultimately we excluded none of the data. Different solutions yielded variations of less than  $0.1 \text{ km s}^{-1}$  in the individual velocity semiamplitudes ( $K_1$  and  $K_2$ ) for individual components, an order of precision which is essential to a reliable analysis of the physical characteristics of a binary (Andersen 1991), since velocity enters as a cube in binary mass determinations (effectively through Kepler's third law).

Since a synchronously rotating star should have  $v \sin i$  of  $15 \text{ km s}^{-1}$ , and since we computed the radial velocities against templates of  $v \sin i = 10$  and  $20 \text{ km s}^{-1}$ , we ran orbital solutions for both sets of radial velocities and later derived masses from both sets of elements (see Sec. 4). The final orbital solution for  $v \sin i = 10$  is shown in Fig. 1; the solution for  $v \sin i = 20$  is virtually indistinguishable at the scale of the graph, except for a few points near the zero-velocity crossing. The adopted solution is shown as a solid line, and the overall fit appears excellent. The rms error of the fit for each component is less than  $1.0 \text{ km s}^{-1}$ , as can be seen in Table 2, where the orbital elements for the spectroscopic solutions are presented.

TABLE 2. Orbital parameters of V505 Per from radial velocity data.

Property	Symbol	Value	
Period	P	4.2220168 days (fixed)	
Epoch (primary minimum)	T <sub>0</sub>	2447808.5994 HJD	
		using template $v \sin i = 10 \text{ km s}^{-1}$	using template $v \sin i = 20 \text{ km s}^{-1}$
Helioc. Velocity of Barycenter	$\gamma$	$+0.040 \pm 0.074 \text{ km s}^{-1}$	$-0.183 \pm 0.085 \text{ km s}^{-1}$
Primary vel. semiamplitude	$K_1$	$88.93 \pm 0.14 \text{ km s}^{-1}$	$88.70 \pm 0.16 \text{ km s}^{-1}$
Secondary vel. semiamplitude	$K_2$	$90.30 \pm 0.14 \text{ km s}^{-1}$	$89.92 \pm 0.15 \text{ km s}^{-1}$
Error in fit to primary data	$\sigma_1$	$0.82 \text{ km s}^{-1}$	$0.97 \text{ km s}^{-1}$
Error in fit to secondary data	$\sigma_2$	$0.84 \text{ km s}^{-1}$	$0.91 \text{ km s}^{-1}$
Sec. to primary mass ratio	$m_2/m_1$	$0.985 \pm 0.002$	$0.986 \pm 0.003$
Projected primary Semiaxis	$a_1 \sin i$ ( $10^9 \text{ m}$ )	$5.163 \pm 0.008$	$5.149 \pm 0.010$
Projected secondary Semiaxis	$a_2 \sin i$ ( $10^9 \text{ m}$ )	$5.242 \pm 0.008$	$5.221 \pm 0.010$
Minimum primary mass	$m_1 \sin^3 i$ ( $M_\odot$ )	$1.268 \pm 0.005$	$1.255 \pm 0.005$
Minimum secondary mass	$m_2 \sin^3 i$ ( $M_\odot$ )	$1.250 \pm 0.004$	$1.238 \pm 0.005$

TABLE 3. The variable and companion stars.

Star	Spectral Type	V	B-V
SAO 023229 (V505 Per)	F5V	6.87	+0.43
SAO 023407 (comparison)	F2V	6.76	+0.38
SAO 023305 (check)	B9V	7.65	+0.05

## 3. PHOTOMETRIC OBSERVATIONS AND ANALYSIS

Differential photometry was carried out by two of the authors (Williams and Agerer) during the interval 1989–1994. Williams, located in Indianapolis, IN, used a 28 cm Schmidt–Cassegrain telescope and an Optec SSP-3 photodiode photometer equipped with *B* and *V* filters matched to the Johnson *B* and *V* system as provided by the manufacturer. Agerer, located in Zweikirchen, Germany, used a 35 cm automated photoelectric telescope equipped with an uncooled EMI 99781 photomultiplier. Standard filters for the Johnson *B* and *V* passbands (1 mm BG12 plus 2 mm GG385 for *B* and 1 mm GG495 for *V*) were used. The comparison star was SAO 23407 and the check star was SAO 23305. Data on the program, check, and comparison stars obtained from Sky Catalog 2000.0 (Hirshfeld & Sinnott 1982) are listed in Table 3.

Observations were corrected for differential airmass effects and transformed to the standard Johnson *UBV* system. Since the comparison star and the variable differ by only 0.05 mag in *B* – *V*, the transformation corrections were very small. A total of 641 observations in *B* and 683 observations in *V* were obtained. These data have been deposited as file number 319E the IAU Commission 27 Archive of Unpublished Photometry. The *B* and *V* light curves are shown in Figs. 2 and 3, with the orbital phase computed from the ephemeris:

$$\text{Min } I = \text{HJD } 2447808.5994 + 4^d.2220168E. \quad (1)$$

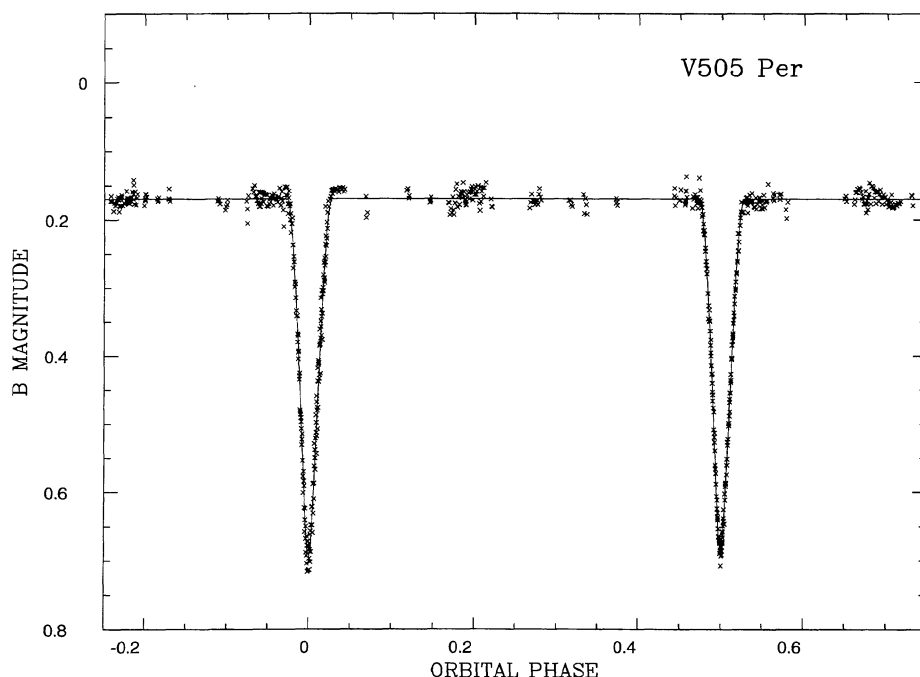
This ephemeris was derived by using the earliest photoelectric time of minimum as the initial epoch and double the value of the period reported by Kaiser *et al.* (1990) from photographic and visual minima times spanning a 50-year interval. Following the completion of the photometric and spectroscopic analysis included in this paper, Williams examined more than 800 Harvard College Observatory sky patrol plates taken between 1900 and 1940, finding 12 earlier times of minimum. Table 4 lists these times, along with new photoelectric times and previously published photoelectric and photographic times of minima covering an interval of 90 years. For computational purposes, we combined the timings of the minima observed in two filters. A least squares solution was then performed, with weights of 1.0 for photoelectric minima and 0.02 for the photographic plate minima, yielding the following improved light elements:

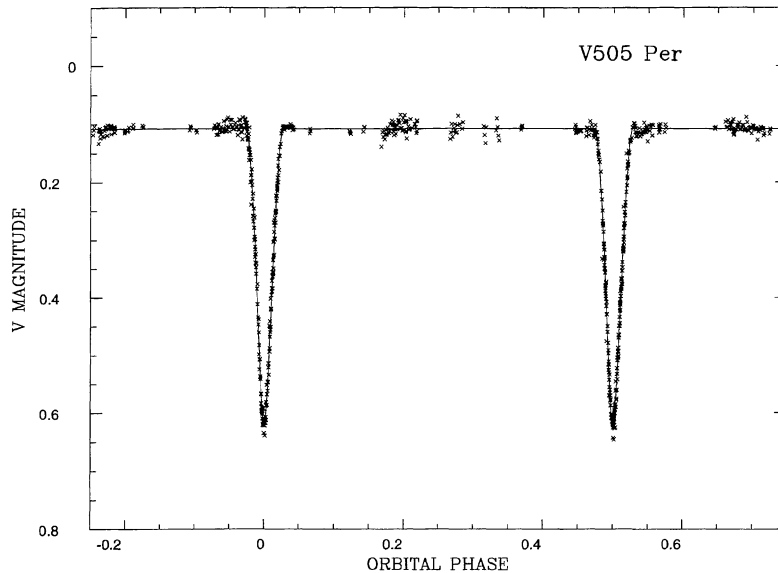
$$\text{Min } I = \text{HJD } 2447808.5998 + 4^d.22201924E. \quad (2)$$

$\pm 1 \qquad \qquad \pm 4$

Because the photoelectric observations used in the light-curve analysis span only 350 orbital cycles since the initial epoch in Eq. (2), the revised period does not introduce a significant difference in the calculated phases or in our analysis of the properties of the system, and we used Eq. (1) for all calculations in this paper. Nevertheless, for future observations of V505 Persei, we advise the use of the revised period.

The photometric data were analyzed using the EBOP program (Popper & Etzel 1981) which incorporates the Nelson–Davis–Etzel model. Because the observed primary and sec-

FIG. 2. The observed light curve in *B* (+ 's) and the fitted model (solid curve).

FIG. 3. The observed light curve in  $V$  (+ 's) and the fitted model (solid curve).

ondary eclipses of V505 Per were very nearly equal in depth, we could assume that the two component stars were nearly identical. We therefore chose identical values of coefficients for limb darkening (Wade & Rucinski 1985) and gravity brightening (Martynov 1973), using our photometric value of  $B-V = +0.43$  to determine an appropriate temperature  $T = 6460$  K (Popper 1980) for our choice of coefficients. These values were  $u_B = 0.66$ ,  $u_V = 0.56$ ,  $y_B = 0.32$ , and  $y_V = 0.56$ . The gravity-brightening coefficients are 1/4 of the radiative values, a figure appropriate for convective envelopes. General solutions were then attempted in which the main variables were the central surface brightness, the radius of the primary, the ratio of the radii, and the orbital inclination. The algorithm converged successfully for both colors. Mean values were then adopted for the geometric param-

eters. Additional light curve solutions were then made to determine consistent values for the radiative parameters. The resultant parameter values and their mean errors are listed in Table 5. The fits to the data are shown in Fig. 2 and 3, and the residuals of the fit are shown in Fig. 4.

#### 4. PHYSICAL PROPERTIES OF THE SYSTEM

The spectroscopic results described in Sec. 2 can be combined with the photometric results described in Sec. 3 to yield the absolute physical properties of the binary star system. We computed masses and radii of the two stars assuming both  $v \sin i = 10 \text{ km s}^{-1}$ , and  $v \sin i = 20 \text{ km s}^{-1}$ . There is a systematic difference of less than 1% between the two solutions, but since the expected  $v \sin i$  is  $15 \text{ km s}^{-1}$ , we have adopted values for mass and radius that are an average of the 10 and  $20 \text{ km s}^{-1}$  solutions. Effective temperatures of the components are based on the color index from the photometry ( $B-V = +0.43$ ) and on the difference in color index derived from the photometric  $B$  and  $V$  orbits. The conversion from color index to effective temperature uses the values in Table 1 of Popper's (1980) review article. The uncertainty in the effective temperature was derived from the uncertainties in the individual color indices of the components.

Our results, listed in Table 6, include the formal values of the standard errors in the solution, but do not include possible systematic errors in scale. We have assumed no inter-

TABLE 4. Minima of V505 Per.

HJD 2440000+	Error	Photographic or Photoelectric	Epoch, Eq.(2)	O-C, Eq.(2)	Source
16468.538	--	pg	-7423.0	-0.013	1
16563.526	--	pg	-7400.5	-0.020	1
16702.838	--	pg	-7367.5	-0.035	1
18277.681	--	pg	-6994.5	-0.005	1
18545.821	--	pg	-6931.0	0.037	1
19381.748	--	pg	-6733.0	0.004	1
20409.849	--	pg	-6489.5	0.043	1
20751.811	--	pg	-6408.5	0.021	1
22197.832	--	pg	-6066.0	0.001	1
28469.632	--	pg	-4580.5	-0.009	1
28564.610	--	pg	-4558.0	-0.026	1
29193.705	--	pg	-4409.0	-0.012	1
29535.713	--	pg	-4328.0	0.012	2
29898.776	--	pg	-4242.0	-0.018	2
30240.798	--	pg	-4161.0	0.020	2
47808.5994	$\pm 0.0006$	pep V	0.0	-0.0004	3
47810.7099	0.0008	pep V	0.5	-0.0009	3
47922.5921	0.0003	pep B	27.0	-0.0022	4
47922.5948	0.0004	pep V	27.0	0.0005	4
48135.8068	0.0015	pep V	77.5	0.0005	1
48190.6934	0.0015	pep B	90.5	0.0009	1
48281.4657	0.0002	pep B	112.0	-0.0003	4
48281.4660	0.0002	pep V	112.0	0.0000	4
48490.4565	0.0003	pep V	161.5	0.0006	5
48490.4571	0.0005	pep B	161.5	0.0012	5
48509.4549	0.0005	pep B	166.0	0.0001	5
48509.4549	0.0006	pep V	166.0	-0.0001	5
49214.5317	0.0006	pep B	333.0	-0.0004	6
49214.5319	0.0014	pep V	333.0	-0.0002	6
49250.4190	0.0002	pep B	341.5	-0.0004	6
49250.4192	0.0002	pep V	341.5	-0.0002	6
49288.4175	0.0004	pep V	350.5	0.0000	6
49288.4180	0.0004	pep B	350.5	0.0005	6

Sources: (1) This paper; (2) Kaiser et al. 1990; (3) Williams et al. 1990; (4) Agerer 1991; (5) Agerer 1992; (6) Agerer 1994

TABLE 5. Photometric orbit of V505 Per.

Parameter	Symbol	B	V	Adopted
Radius of Primary	$r_p$	$0.0868 \pm 0.0022$	$0.0853 \pm 0.0023$	$0.0861 \pm 0.0022$
Ratio of Radii	$k$	$0.96 \pm 0.05$	$1.00 \pm 0.05$	$0.98 \pm 0.05$
Orbital Inclination	$i$	$87.84^\circ \pm 0.03^\circ$	$87.82^\circ \pm 0.02^\circ$	$87.83^\circ \pm 0.02^\circ$
Secondary Surface Brightness	$J_s$	$0.988 \pm 0.005$	$1.000 \pm 0.004$	
Luminosity of Primary	$L_p$	$0.512 \pm 0.023$	$0.505 \pm 0.022$	



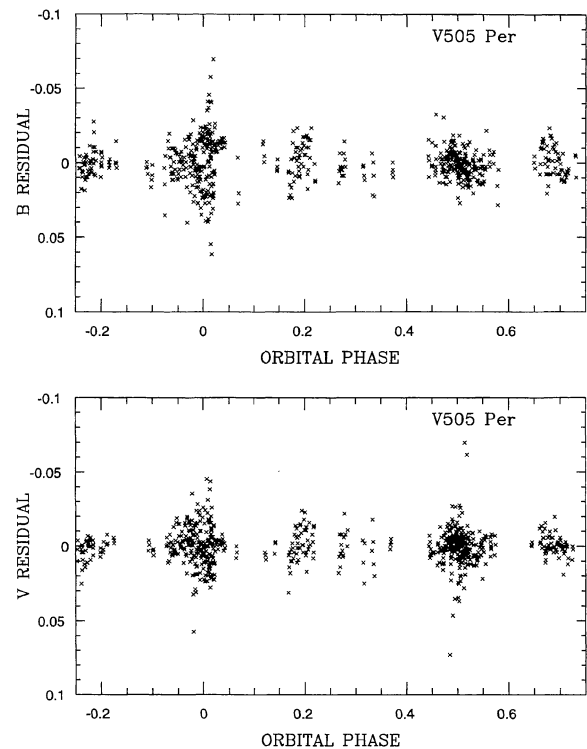


FIG. 4. Residuals from the fitted model in *B* and *V*.

stellar reddening in this case because the star is relatively nearby.

That the two components of V505 Per are not identical is evident from the difference in the depths of primary and

TABLE 6. Absolute properties of V505 Per.

Property	Symbol (units)	Primary	Secondary
Mass	$M(\text{solar})$	$1.265 \pm 0.006$	$1.247 \pm 0.006$
Radius	$R(\text{solar})$	$1.29 \pm 0.03$	$1.27 \pm 0.07$
Surface Gravity	$\log g \text{ (cgs)}$	$4.32 \pm 0.02$	$4.33 \pm 0.04$
Temperature	$\log T \text{ (K)}$	$3.812 \pm 0.007$	$3.805 \pm 0.009$
Surface Brightness	$F_v$	$3.809 \pm 0.008$	$3.802 \pm 0.010$
Bol. Absolute Mag.	$M_{\text{bol}}$	$3.58 \pm 0.07$	$3.69 \pm 0.09$
Vis. Absolute Mag.	$M_v$	$3.61 \pm 0.08$	$3.72 \pm 0.10$
Luminosity	$\log L(\text{solar})$	$0.42 \pm 0.05$	$0.38 \pm 0.08$
Distance	$d(\text{parsecs})$		$62 \pm 3$
Difference in B-V	$\Delta(B-V)$		$0.03 \pm 0.03$

secondary eclipses, and from the small but significant differences in the velocity semiamplitudes of the two stars. The resulting masses and radii, consequently, differ by about 1.5%.

These observational results can be compared with those of stellar structure theory, such as those of Hejlesen (1980) or Mengel *et al.* (1979). Figure 5 shows how the masses of V505 Per compare with other observations and with theory. The agreement with observations of similar systems compiled by Popper (1980) and Lacy (1992) seems quite good. Comparison with isochrones of Mengel for a chemical composition of  $Y = 0.27$  and  $Z = 0.03$  near zero age also seems quite good, as does the agreement with  $\log(\text{Age}) = 6.6$  isochrone for  $Y = 0.28$  and  $Z = 0.02$  from Bertelli *et al.* (1994). The binary star V505 Per therefore appears to be somewhat above the zero-age main sequence, indicating some evolution has taken place.

Assuming solar abundances, the age of V505 Per can be estimated by comparison with the Bertelli isochrones. Figure

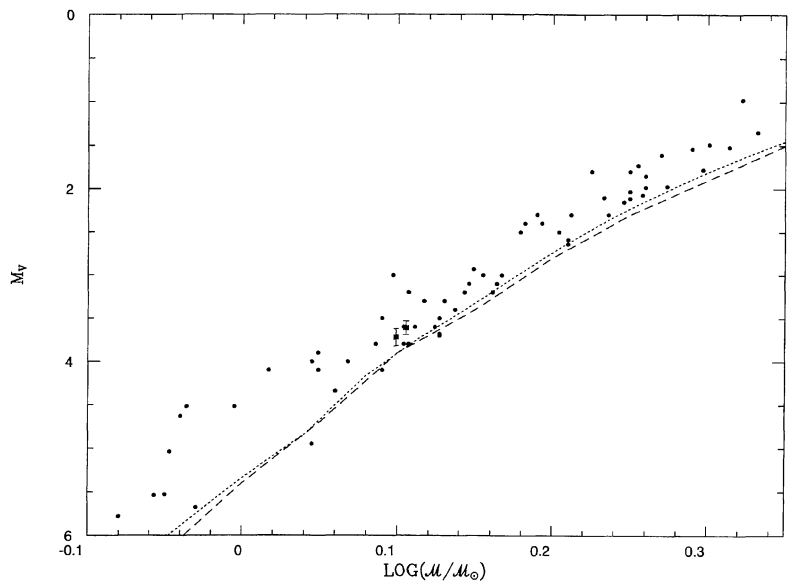


FIG. 5. Absolute visual magnitude versus mass for eclipsing binary stars listed by Popper (1980) and Lacy (1992) shown as solid dots. The components of V505 Persei are shown as crosses. ZAMS lines are shown from models by Mengel (1979) (dotted line), calculated for  $Y = 0.27$  and  $Z = 0.03$ , and by Bertelli *et al.* (1994) (dashed line), calculated for  $Y = 0.28$  and  $Z = 0.02$ .

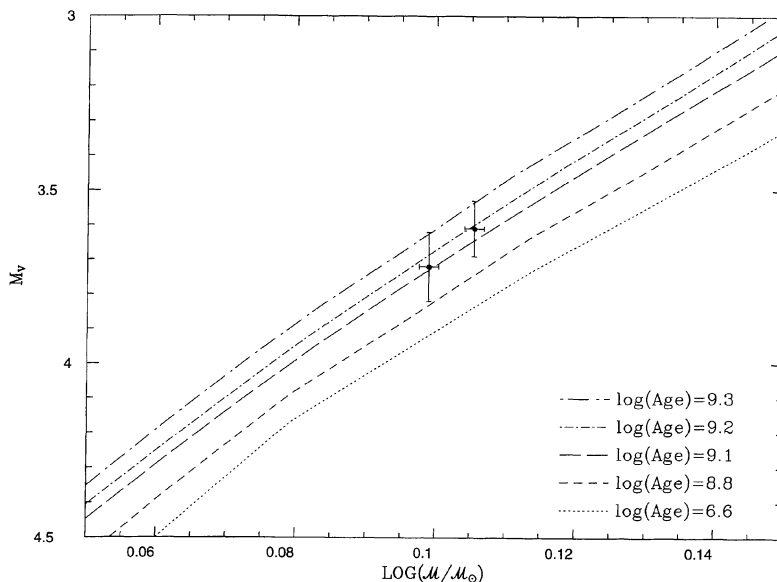


FIG. 6. Comparison of the observed mass and luminosity of the two components of V505 with isochrones of various age by Bertelli *et al.* (1994), calculated for  $Y = 0.28$  and  $Z = 0.02$ .

6 shows this comparison for isochrones with  $Y = 0.28$  and  $Z = 0.02$ . The components seem to align nicely with the slope of the theoretical isochrones in the mass-luminosity plane, indicating a  $\log(\text{Age})$  of  $9.15 \pm 0.15$  (i.e.,  $1.4 \times 10^9 \pm 0.4 \times 10^9$  years). Further work to reduce the uncertainty in the derived values of  $M_v$ , along with an abundance analysis of the stellar spectrum to define the appropriate theoretical isochrones, could refine the precision of this age determination.

Thanks to Dave Latham for advice and support in observing; to CfA observers Joe Caruso and Joe Zajac; to Bob Davis for maintaining the CfA database and obtaining additional observations; to Doug Mink for software help; to Bruce Hrivnak for several confirming radial velocity measurements; to Mike Seeds and Harold Nations for helpful discussions; to Martha Hazen for access to the Harvard Plate Stacks. L.A.M. was supported in part by grants from Gettysburg College.

#### REFERENCES

- Agerer, F. 1991, BAV Mitteilungen No. 59  
 Agerer, F. 1992, BAV Mitteilungen No. 60  
 Agerer, F. 1991, BAV Mitteilungen No. 68  
 Andersen, J. 1991, ARA&A, 3, 91  
 Bertelli, G., Bressan, A., Chiosi, C., Fagotto, F., & Nasi, E. 1994, A&AS, 106, 275  
 Hejlesen, P. M. 1980, A&AS, 39, 347  
 Hirshfeld, A., & Sinnott, R. W. (ed.) 1982, Sky Catalog 2000 (Cambridge University Press, Cambridge)  
 Kaiser, D. H. 1989, J. Am. Assoc. Var. Star. Obs., 18, 149  
 Kaiser, D. H., Baldwin, M. E., and Williams, D. B. 1990, Inf. Bull. Var. Stars, No. 3442  
 Kurtz, M. J., Mink, D. J., Wyatt, W. F., Fabricant, D. G., Torres, G., Kriss, G. A., & Tonry, J. L. 1992, in Astronomical Data Analysis Software and Systems I, ASP Conf. Ser. 25, edited by D. M. Worral, C. Biemsterfer, and J. Barnes (ASP, San Francisco), p. 432.1  
 Lacy, C. H. 1992, AJ, 104, 801  
 Latham, D. W. 1985, in Stellar Radial Velocities, Proc. IAU Coll. 88, edited by A. G. D. Philip and D. W. Latham (Davis, Schenectady), p. 21  
 Latham, D. W. 1992, in Complementary Approaches to Binary and Multiple Star Research, Proc. IAU Coll. 135, edited by H. McAlister and W. Hartkopf, ASP Conf. Ser. 32 (ASP, San Francisco), p. 110  
 Latham, D. W., Nordström, B., Andersen, J., Torres, G., Stefanik, R., Thaller, M., & Bester, M. 1996, A&A, 314, 864  
 MacRobert, A. 1990, S&T, 79, 189  
 Marschall, L. A., Stefanik, R. P., Nations, H. L., & Davis, R. J. 1990, Inf. Bull. Var. Stars, No. 3447  
 Martynov, D. Y. 1973, in Eclipsing Variable Stars, edited by V. P. Tsevevich (Halsted, New York), p. 146  
 Mathieu, R. 1994, ARA&A, 32, 465  
 Mazeh, T., & Zucker, S. 1994, ApJ, 420, 806  
 Mengel, J. G., Sweigart, A. V., Demarque, P., & Gross, P. G. 1979, ApJS, 40, 733  
 Popper, D. M. 1980, ARA&A, 18, 115  
 Popper, D. M., & Etzel, P. B. 1981, AJ, 86, 102  
 Wade, R. A., & Rucinski, S. M. 1985, A&AS, 60, 471  
 Williams, D. B., Landis, H. J., & Pray, D. 1990, Inf. Bull. Var. Stars, No. 3479